Electrical Characterization of Epitaxial Layers of Gallium Arsenide

Rani Khatwani
M.Sc Physics, University of Bombay, India, 1982

A thesis submitted to the faculty
of the Oregon Graduate Center
in partial fulfillment of the
requirements for the degree
Master of Science
in
Electrical Engineering

December, 1988

The thesis "Electrical Characterization of Epitaxial Layers in Gallium Arsenide" by Rani Khatwani has been examined and approved by the following Examination Committee.

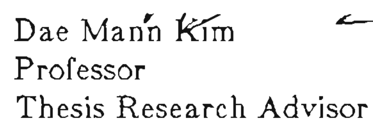

Dae Mann Kim
Professor
Thesis Research Advisor

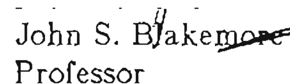

John S. Blakemore
Professor

Raj Solanki
Associate Professor

Carl Clawson
Engineer, Advanced Sys. Concept Inc.

To My Parents

Acknowledgements

I am grateful to my thesis advisor Dr. Kim for his support and encouragement during the course of this work.

I wish to thank my thesis committee Dr. John Blakemore, Dr. Raj Solanki and Dr. Carl Clawson for their time and co-operation. Special thanks to Carl for his careful reading of my thesis and his valuable suggestions. I am also thankful to him for his guidance during the course of this work.

My deepest gratitude to Charles Bickford for letting me use his equipment. Charles and Carl taught me how to use the equipment and provided assistance whenever I needed. I am indebted to them for all their help. Thanks are also due to Jan Boman for providing me with the GaAs samples.

I am also grateful to my friend, Nitin Borkar, for all the encouragement and help during this period.

Finally, I am obliged to my parents for their love and support throughout my career.

Table of Contents

Introduction 1

Epitaxial Growth Method 3

Growth Techniques 3

Organo-Metallic Chemical Vapor Phase Epitaxy 4

Electrical Characterization Techniques 10

Hall Effect Measurements 10

Carrier Concentration Versus Temperature Analysis 12

Electron Mobility in GaAs 15

Ionized Impurity Scattering 17

Neutral Impurity Scattering 18

Deformation Potential Scattering 20

Polar Mode Optical Scattering 21

Characterization Results 22

Experimental Details 22

Epilayer Thickness Measurement 22

Mobility and Carrier Concentration 23

Results and Discussion 24

Growth Properties 24

Conclusion 38

References 40

Appendix A 44

Vita 54

List of Tables and Figures

Table I 8

Table II 25

Table III 26

Table IV 36

Figure 1 28

Figure 2 30

Figure 3 31

Figure 4 34

Figure 5 35

Figure 6 37

ABSTRACT

ELECTRICAL CHARACTERIZATION OF EPITAXIAL LAYERS OF GALLIUM ARSENIDE

Rani Khatwani, M.S.
Oregon Graduate Center, 1988

Supervising Professor: D. M. Kim

Epitaxial layers of Gallium Arsenide are grown by organo-metallic chemical vapor phase epitaxy (OMVPE) involving a reaction of arsine and trimethylgallium. These layers are doped n-type with silane.

The Hall Coefficient and mobility have been measured in n-type epitaxial gallium arsenide from 365 K to 15 K, and impurity concentrations were computed from the results. Mobilities up to 3745 $cm^2V^{-1}sec^{-1}$ at 300 K and 11330 $cm^2V^{-1}sec^{-1}$ at 77 K have been measured.

The techniques for determining the concentrations of donors and acceptors in semiconductor samples from Hall effect and resistivity measurements are described. Analyses of the temperature variation of the carrier concentration and mobility permit the determination of N_D and N_A.

The separate contributions to carrier scattering have been evaluated. Polar scattering is apparently dominant down to about 100 K. Piezoelectric scattering and deformation potential scattering are significant at 77 K. The Brooks-Herring theory of ionized impurity scattering is shown to give good quantitative agreement with results at low temperatures.

CHAPTER 1

INTRODUCTION

As a starting material for semiconductor fabrication, Gallium Arsenide (GaAs) offers, in principle, considerable advantages over silicon. Firstly, the electron mobility is higher in GaAs than in silicon implying that fast switching components working at tens of GHz are possible. GaAs devices are thus important for digital circuits and for linear applications in monolithic microwave integrated circuits (MMIC) such as satellite communication.

Of equal importance and increasing interest is the role of GaAs in heterostructure devices, both electronic and electron-optic and the obvious possibility of merging these applications in a single chip. To produce devices of high performance over the whole doping range, material must be provided in which the impurity content is carefully controlled.

Organo-metallic chemical vapor phase epitaxy (OMVPE) was used to grow layers of GaAs on GaAs and GaAs on AlGaAs. Electrical characterization of these layers was performed using Hall measurements and Secondary Electron Mass Spectrometry (SEM).

The OMVPE technique, described in detail in chapter II, has become an important technique in recent years because of its suitability for large scale production. The process has become an important III-V epitaxial growth technology for electronic and opto-electronic devices. Since the first demonstration of OMVPE for GaAs by Manasevit [1], work has included efforts to improve the quality of the material and utilize it in state-of-the-art devices. Areas of major success have been solar cells, heterojunction lasers, quantum well structures and FET's. A major disadvantage of OMVPE, however, is that the growth process depends on chemistry and fluid dynamics that are difficult to understand.

The various characterization techniques used for the grown epilayers are described in chapter III. Also described in this chapter is the theory of the different scattering mechanisms that are important in GaAs. The results and conclusion from the present work are described in chapter IV and V. Detailed derivations of some of the equations used in this work are given in the appendixes.

CHAPTER 2

Epitaxial Growth Method

2.1. Growth Techniques

The GaAs epitaxial layers are grown by several techniques. The major ones include Molecular Beam Epitaxy (MBE), Liquid Phase Epitaxy (LPE) and Vapor Phase Epitaxy (VPE). MBE is the growth of elemental, compound and alloy semiconductor films by the impingment of directed thermal-energy atomic or molecular beams on a crystalline surface under ultra-high-vacuum conditions. LPE, on the other hand, depends on the fact that the solubility of arsine in gallium-rich solutions decreases with decreasing temperature. Included within the family of vapor phase epitaxial growth techniques are two methods, namely : (1) chloride transport and (2) organo-metallic chemical vapor phase epitaxy (OMVPE). In the chloride transport system, gallium is transported in the form of gallium chloride ($GaCl_3$) and reacted with arsenic. Growth is carried out in a hot-wall quartz reactor in a flowing H_2 ambient. OMVPE growth of GaAs involves the pyrolysis of a vapor phase mixture of arsine and most commonly, trimethylgallium (TMG) or triethylgallium (TEG). None of the three methods just listed meets all compound sem-

iconductor epitaxial needs but a comparison of the three reveals the growing importance of OMVPE.

2.2. Organo-Metallic Chemical Vapor Phase Epitaxy

OMVPE has become an important method in recent years for the growth of high quality epitaxial layers of various III-V semiconductor materials. The controllability, reproducibility, and good uniformity of OMVPE make it useful for fabricating highly advanced structures. In particular, the use of such layers for optoelectronic, microwave and high speed digital circuits has given promising results. This technique has also produced layers approaching the purity and mobility of the best layers grown by the halide or hydride techniques, and has generated much interest due to its simplicity and flexibility.

Current OMVPE applications can be placed in two categories :

(a) Production-scale fabrication of established optoelectronic, microwave and electronic devices - For example, OMVPE is used in production today to produce high quality films for photovoltaic, microwave and analog devices.

(b) MBE-alternative R & D for leading edge compound semiconductor device structures - Much of the research being done today with compound semiconductor device structures involves FETs based on submicron-thick layers. With OMVPE it is possible to grow films

less than 100 Å thick with interface between layers that approach a few atomic layers.

The first description of the OMVPE process can be traced to Manasevit and coworkers [2]. He wished to emphasize that, this process, which was then a new concept, transported metals using organic compounds, hence "metalorganic". rather than the more rigorously correct "organometallic". Other authors have used alternative nomenclatures including OMVPE (organometallic vapor phase epitaxy), OMCVD (organometallic chemical vapor deposition), OMP (organometallic pyrolysis), and probably others. Regardless of the name, the point of commonality is that temperature controlled vapors of organometallic compounds are used to transport at least one of the primary film constituents.

Manasevit's work [1, 3-6] dealt primarily with deposition on insulating substrates such as glass, sapphire, beryllium oxide, and thorium oxide. Manasevit [3] demonstrated that triethylgallium (TEG) and Arsine (AsH_3) deposited single-crystalline GaAs pyrolytically in an open tube reactor. During the same time frame, Rai-Choudhury [7], produced single crystal GaAs on GaAs substrates. Thomas [8] grew gallium phosphide (GaP) from TEG and triethylphosphorus (TEP). Ito et al. [9] discovered that the GaAs carrier background changes from p to n type

as the $[AsH_3]/[TMG]$ ratio is increased, and Seki et al. [10] settled doubts about the ability of OMVPE to produce high-purity GaAs by growing films with $n = 7 \times 10^{13} cm^{-3}$ and $\mu_{77} = 120{,}000\ cm^2/Vs$

OMVPE has demonstrated the capability to grow the widest variety of III-V materials, of all the alternative epitaxial techniques. Monolayer thickness and transitions [11-13] are possible. The process is also potentially scalable to large-area production. The most important capability, perhaps, to be fully exploited, is the ability to grow several different III-V alloy systems in the same physical apparatus, in any sequence, during a single deposition run.

In a typical metalorganic reaction, gallium arsenide is grown by metering trimethylgallium (a group III alkyl) and arsine (a group V hydride) into a reactor:

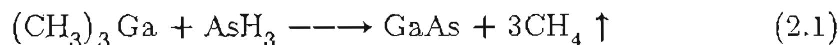

$$(CH_3)_3Ga + AsH_3 \longrightarrow GaAs + 3CH_4 \uparrow \qquad (2.1)$$

This reaction is a pyrolysis of the vapor phase mixture of the reactants in the temperature range of 600 °C to 800 °C; the reactants crack and the gallium and arsenic elements diffuse through the boundary layer in the reaction chamber to combine at or near a heated substrate. This is most interesting when it results in deposition on a suitable single crystal substrate, such as GaAs, forming an epitaxial layer.

A number of attractive features are associated with the OMVPE process. All constituents are in the vapor phase allowing for accurate electronic control of important system parameters, such as gas flow rates. The pyrolysis reaction is relatively insensitive to temperature, allowing for efficient and reproducible deposition of very thin layers with abrupt interfaces between layers. Complex multiple layer heterostructures can be grown utilizing computer controlled gas exchange systems.

The epitaxial growth of GaAs to be reported on here was grown at Tektronix in a computer controlled OMVPE Thomas Swan reactor (Epitor 04). Trimethylgallium, $(CH_3)_3Ga$, and arsine, AsH_3 , were used for deposition of GaAs on semi-insulating substrates. The crystal orientation was (100). The substrate was heated via an infrared lamp. The deposition took place at atmospheric pressure with growth temperatures ranging from 650 °C to 750 °C . The non-doped wafers are usually n-type when the $[AsH_3]/[TMG]$ mole fraction is high and p-type when it is low [14]. To obtain n-type material , silicon doping was used. Depending on the growth conditions, the carrier densities range from 4.217×10^{15} to $1.583 \times 10^{18} cm^3$.

The samples used for this work are listed in table I. In a series of experiments, the effect of change of $[AsH_3]/[TMG]$ mole fraction,

the effect of growth temperature on mobility and the effect of doping

TABLE I

OMVPE RUN #	GROWTH TEMP. $T^{0}C$	SILANE/III (moles/cc)	MARKER LAYER	V/III
79	750	0.16e-2	AlGaAs	30
80	650	0.18e-3	AlGaAs	30
81	750	0.16e-2	-	30
82	750	0.41e-2	-	30
83	650	0.16e-2	-	30
96	750	0	AlGaAs	30
99	750	0	AlGaAs	30
100	750	0.36e-2	AlGaAs	30
101	680	0	AlGaAs	15
102	680	0	-	15
104	750	0	AlGaAs	30
108	680	0	AlGaAs	15
112	680	0.45e-2	AlGaAs	15
113	680	0.81e-3	AlGaAs	15

concentration on mobility were investigated.

In the case of organo-metallic vapor phase epitaxy the growth rate of epitaxial layers is virtually independent of temperature within a certain range and arsine concentration but varies linearly with the TMG concentration. Several workers since Manasevit and Simpson [1] confirmed that the controlling factor in the growth rate is probably the diffusion of TMG through the thin stagnant layer of gas [15] adajacent to the substrate.

CHAPTER 3

Electrical Characterization Techniques

Electrical characterization is a simple approach used to obtain information about the purity of epitaxial layers. Such information is important for the evaluation and control of crystal growth procedures used to prepare high quality epitaxial material for device applications [16]. It is also important for the detailed characterization of epitaxial material in conjunction with other evaluation procedures. Included under the term electrical characterization procedures are Hall coefficient and resistivity measurements, capacitance-voltage measurements, photoconductivity, photo-Hall and photo-capacitance measurements.

3.1. Hall Effect Measurements

Hall-effect measurements have long been a standard technique for obtaining in a relatively simple and reliable manner the carrier concentration and mobility of a semiconductor material. Often no more than the carrier concentration and mobility is required but the Hall data can also be analyzed to provide the concentration of donor and acceptor impurities. To do this it is necessary to fit the experimental mobility versus temperature curve to a theoretical expression and there has been much theoretical effort in the past devoted to the derivation of accurate

values of the carrier mobility [17].

The use of Hall mobility measurements to characterize the electrical properties of GaAs has been a subject of considerable interest [18-23]. Two techniques are most commonly used in the characterization of n-type GaAs. One is to analyze the temperature dependence of the carrier concentration and the other is to analyze the Hall mobility in terms of the relevant scattering mechanisms. The first technique can be used for GaAs with donor concentration upto about $5 \times 10^{15} cm^{-3}$. Beyond this point no donor deionization is observed and the second approach must be used, but this is complicated by the fact that over a considerable range of temperatures and impurity concentrations the mobility is influenced by scattering from longitudinal optical phonons.

To more easily determine the ionized impurity concentration in GaAs, one often used approach has been to simply ignore these complications due to polar mode scattering. In this method an assumed lattice scattering limit is simply combined with the Brooks-Herring [23] mobility formula for ionized impurity scattering and the ionized impurity density is determined from an experimental mobility at some convenient temperature such as 77 K [24-26]. Unfortunately, this can result in large errors especially in the intermediate concentration region. Another approach has been to analyze the experimental mobility with the

Brooks-Herring formula at some fixed lower temperature such as 20 K, where the effects of polar mode scattering should be negligible [27]. For samples with high impurity concentrations, this approach is complicated by the fact that at low temperatures the measured mobility should be lower than that expected from ionized impurity scattering due to the effects of hopping, impurity-band, or degenerate conduction. Also for samples with low impurity concentrations the low temperature mobility may be lower because of neutral impurity scattering or scattering from planar or linear defects. Since these low temperature effects decrease with increasing temperature while lattice scattering increases with increasing temperature there should exist an optimum temperature at which to apply the Brooks-Herring ionized impurity analysis where the effects of these other mechanisms are minimal. Thus, an analysis of the mobility at different temperatures using the Brooks-Herring equation should determine this optimum temperature and establish a more accurate value for the ionized impurity density of a sample.

3.2. Carrier Concentration Versus Temperature Analysis

The parameters determined from the Hall experimental measurements are the Hall coefficient and resistivity, while the quantities of interest for the determination of the electrically active impurity concentrations are the free carrier concentration and the free carrier mobility.

The carrier concentration n is determined from the measured Hall coefficient R_H using the expression

$$n = \frac{r_H}{eR_H} \tag{3.1}$$

where r_H is the Hall coefficient factor. The Hall coefficient factor, was assumed to be unity. The Hall coefficient factor r_H is in general a function of the magnetic field used for the measurement as well as of the sample degeneracy and temperature. The approximation of $r_H = 1$ is good for polar scattering, but at low magnetic fields r_H would be rather greater than unity when ionized impurity scattering is dominant. However, the high carrier mobilities combined with the reasonably high field of 5 kG closely approach the high magnetic field region conditions [28], where r_H becomes unity and independent of the scattering mechanism. The use of a high field will therefore minimize the error introduced by the assumption that $r_H = 1$. Nevertheless, in most reported analyses of Hall coefficient and mobility data to determine the ionized impurity concentration of epitaxial layers, it is assumed that $r_H = 1$.

To determine the donor and acceptor concentrations from the temperature variation of the carrier concentration, a theoretical carrier concentration equation must be fitted to eqn. (3.1). For a non-degenerate n-type semiconductor with a shallow donor concentration N_D and accep-

tor concentration N_A, the concentration n_0 of free electrons in the conduction band is given by [16]

$$\frac{n_0(n_0 + N_A) - n_i^2}{N_D - N_A - n_0 + (n_i^2/n_0)} = \frac{N_c}{g_1} \exp(-E_D/kT) \qquad (3.2)$$

where N_c is the effective density of states of the conduction band, N_D and N_A, respectively, are the donor and acceptor concentrations, E_D the ionization energy of the donors and g_1 is the degeneracy of the donor level. A detailed derivation of eqn.(3.2) is given in Appendix (A).

In particular temperature ranges, it is possible to approximate eqn.(3.2) by simpler relations, and these approximations have been utilized by some workers to estimate the donor and acceptor concentrations without resorting to a detailed fit of the theoretical equation to the experimental data :

(a) at very low temperatures, where $n_0 << N_A$, $N_D - N_A$ and $p_0 = n_i^2/n_0 \approx 0$

$$n_0 \approx \frac{N_c}{g_1} \frac{(N_D - N_A)}{N_A} \exp(-E_D/kT) \qquad (3.3)$$

(b) at slightly higher temperatures or for low values of N_A, where $n_0 >> N_A$ and $p_0 \approx 0$

$$n_0 \approx \left\{ \frac{N_c}{g_1} (N_D - N_A) \right\}^{1/2} \exp(-E_D/2kT) \qquad (3.4)$$

(c) at still higher temperatures (exhaustion region), where $E_D << kT$ but $n_0 >> n_i$

$$n_0 \approx N_D - N_A = \text{constant} \tag{3.5}$$

Simple estimates can be made of E_D and $(N_D - N_A)/N_A$ from the plot of experimental carrier concentration versus $1/T$. Using the value of $n_0 = N_D - N_A$ in the exhaustion temperature range, the donor and acceptor concentrations can both be determined. This procedure has the advantage of being simple, but it generally neglects the temperature dependence of N_C. For GaAs with N_D - N_A in the range 10^{14} - 10^{16} cm^{-3}, this can introduce considerable error.

Eqns. (3.1) and (3.2) have been used successfully by several workers for the analysis of high purity GaAs Hall coefficient data. Bolger et al. [29, 30] used these equations, neglecting the terms involving n_i^2 and assuming $r_H = 1$, to analyze Hall coefficient data taken at a magnetic field of 5 kG with good results. The value used for m_D^* was 0.072m, and the value used for the degeneracy factor g_1 was 2. Stillman et al. [31] also used these same equations and values for r_H, m_D^* and g_1 for the analysis of Hall coefficient data taken at a magnetic field of 5 kG.

3.3. Electron Mobility in GaAs

The electron mobility in doped semiconductors, has been the center of attraction of many investigations, both experimental as well as

theoretical. The scattering mechanisms which determine the transport properties of GaAs were originally examined by Ehrenreich [32] who showed that a combination of polar optical phonon and ionized impurity scattering yielded qualitative agreement with the temperature and impurity concentration dependence of the electron mobility for the purest bulk GaAs.

The electron scattering mechanisms are conveniently divided into two categories, involving the lattice and impurities.

The lattice scattering mechanisms that must be considered are piezoelectric, deformation potential, polar and non-polar optical mode scattering. Of these, the first two involve acoustical phonons and the last two involve optical phonons. Piezoelectric and polar scattering, in particular, occur in the III-V compounds but not in Ge and Si.

Taking into consideration all the scattering mechanisms, the effective relaxation time is given by

$$\frac{1}{\tau(x)} = \sum_{i} \frac{1}{\tau_i(x)} \tag{3.6}$$

where, $\tau_i(x)$ are the relaxation times for the individual scattering processes. The sum is over all the scattering processes and x is the electron energy in units of kT. Using classical statistics, the average relaxation time $<\tau>$ is given by:

$$<\tau> = \frac{4}{3\pi^{1/2}} \int_0^\infty \tau(x) x^{3/2} \exp(-x) dx \qquad (3.7)$$

and the electron mobility is then determined from $\mu = \frac{e<\tau>}{m^*}$, where e is the electronic charge and m^* is the electron effective mass.

3.3.1. Ionized Impurity Scattering

The scattering of electrons by singly ionized impurities is described by the Brooks-Herring equation [23] which takes into account screening of the scattering potential.

Impurities different in valence from the host lattice give rise to (long range) coulomb fields in the semiconductor with a potential of the form $V(r) = e^2/\epsilon r$, where ϵ is the macroscopic dielectric constant. Since the total scattering cross-section of a coulomb charge diverges due to the long range character of the potential, proper care should be taken in screening the bare charge or to "cut-off" the coulomb field of the impurity at some distance.

Brook and Herring introduced a shielding factor into the potential. This arises from the fact that the other electrons in the conduction band redistribute themselves around the impurity in such a way as to cancel its field at large distances.

The Brooks-Herring equation for the ionized impurity scattering mobility μ_I is

$$\mu_I = \frac{3.28 \times 10^{15} (m/m^*)^{1/2} \epsilon^2 T^{3/2}}{(2N_A + n)\left\{\ln(b+1) - b/(b+1)\right\}} \mathrm{cm}^2 \mathrm{V}^{-1} \mathrm{sec}^{-1} \tag{3.8}$$

where,

$$b = \frac{1.29 \times 10^{14} (m^*/m) \epsilon_0 T^2}{n^*} \tag{3.9}$$

and n^* is an effective screening density :

$$n^* = n + \frac{(n + N_A)(N_D - N_A - n)}{N_D} \mathrm{cm}^{-3}$$

3.3.2. Neutral Impurity Scattering

Another important source of resistivity at low temperatures is the scattering due to neutral impurity atoms which must be considered particularly in the case of semiconductors showing a small degree of ionization. Although neutral impurities may be expected to contribute less to the scattering than ionized impurities, their effect may not be by any means negligible, particularly at low temperatures. At such temperatures they may far out number the ionized impurities.

It was first pointed out by Bardeen and Pearson [33] that neutral donors, owing to the large orbit of the bound electron, could present a rather large cross section for scattering in which the bound and free

electron exchange places. A strictly analogous effect occurs in the scattering of electrons by hydrogen atoms. The effect has been studied by Erginsoy [34] who gives the formula

$$\frac{1}{\tau_{NI}} = \frac{\pi m_c}{10 N_N h a_d} \tag{3.10}$$

where, a_d is the radius of the hydrogenic orbit of the bound electron on the impurity, and N_N is the number of neutral impurities per cubic centimeter. Thus, from Erginsoy's model, the neutral impurity scattering mobility is given by

$$\mu_{NI} = \frac{4\pi^2 \epsilon\epsilon_0 \epsilon_d}{5 e h N_N} \tag{3.11}$$

where, ϵ is the effective dielectric constant and ϵ_d is the binding energy for temporary association of an electron with a neutral donor atom. Eqn (3.11) has no explicit temperature dependence, however N_N may vary with T.

It should be noted here that the neutral impurity scattering is proportional to the dielectric constant, while ionized impurity scattering is inversely proportional to the square of the dielectric constant. Thus neutral impurity scattering becomes of much greater importance in high dielectric constant semiconductors. Neutral impurity scattering is independent of the temperature and also does not vary with the energy of the incident electron or hole. Hence its importance at very low

temperatures when $n << N_N$, i.e., when almost all impurities are unionized. This scattering process has an appreciable effect on the resultant mobility only for relatively uncompensated samples at low temperatures.

3.3.3. Deformation Potential Scattering

In a rather pure crystal of a semiconductor which is bound together primarily by covalent forces, electrons are scattered predominantly by longitudinal acoustic phonons. The passage of a longitudinal vibration through a crystal gives rise to alternate regions of compression and extension of the crystal lattice which create a local modulation of the dielectric constant and of the energies ϵ_c and ϵ_v which describe the upper and lower limits of the intrinsic gap. Such dialation variations affect ϵ_c to an extent measured by the deformation potential :

$$E_1 = -V\left(\frac{dE_c}{dV}\right) \tag{3.12}$$

It was shown by Shockley and Bardeen [35] that LA phonons would scatter electrons isotropically for most of the temperature range. They expressed the free path between electrons in terms of the deformation potential as :

$$\lambda = \frac{4\rho {v_{LA}}^2}{k_0 T}\left(\frac{h^2}{2m_c E_1}\right)^2 \tag{3.13}$$

where, ρ is the density of the material, E_1 is the deformation potential,

v_{LA} is the speed of the long wave LA phonons. The mobility for this scattering mechanism is given by:

$$\mu_L = \frac{e\hbar^4 \rho\, v_{LA}{}^2}{6\pi^2 m_c E_1{}^2 (2\pi m_c kT)^{3/2}} \tag{3.14}$$

3.4. Polar Mode Optical Scattering

Another scattering mechanism for electrons and holes, particularly at reasonably high temperatures and in partially ionic lattices, is that effected by optical mode phonons. Whereas accoustic mode phonons mostly have an energy which is very small compared with that of the electrons they scatter, optical mode phonons have a large energy $\hbar w_{opt}$ regardless of their wave-vector.

Polar mode scattering is unimportant at low temperatures, but it can become predominant in some materials when $k_0 T$ becomes comparable with the formation energy $\hbar w_{opt}$ of optical phonons.

Various models suggest that

$$\mu_{OM} \propto [\exp(\hbar \nu_{LO}/kT) - 1] \tag{3.15}$$

where, ν_{LO} is the LO phonon frequency.

CHAPTER 4

Characterization Results

4.1. Experimental Details

The epitaxial growth of a suitably doped, single crystal layer forms the starting point for many commonly used microcircuit fabrication techniques. Since the entire microcircuit is eventually fabricated within this layer, it is necessary to evaluate such layer parameters as resistivity, mobility, carrier concentration and thickness.

4.1.1. Epilayer Thickness Measurement

Two methods were used to measure the thickness of epitaxial layers. Both the methods involved selective etching of the substrate.

For layers with the AlGaAs marker layer, delineation was achieved using a 3:1 water and clorox solution. Growing a layer of AlGaAs as a marker layer over the substrate permitted thickness measurements of the top layer after delineation. The samples were cleaved after growth and selected samples were delineated using the clorox solution for 10 seconds. A SEM session (at Tektronix) was scheduled directly after the Cambridge 240 SEM had been calibrated with 5 μm latex spheres. The results indicated a useful measuring technique that is repeatable.

For the layers without the AlGaAs marker layer, the following method was used for thickness measurement. The etchant used was potassium ferricyanide. Freshly cleaved samples were delineated in a solution of potassium ferricyanide for 12-15 seconds and then rinsed in water. They were then mounted on a small piece of microscope slide using clay and mounted under the Zeiss light microscope. Thickness measurements were then made with the eyepiece scale which was calibrated with a variety of millimeter scale rules.

4.1.2. Mobility and Carrier Concentration

Gallium arsenide is usually compensated. Here the mobility and the carrier concentration in an epitaxial layer may be separately determined by means of the Hall effect.

The experimental techniques used for the measurement of the Hall coefficient and resistivity of semiconductor samples are well known. Since the donor ionization energy (≈5meV) in GaAs is rather small, one must make Hall measurements well below 15 K to accurately determine donor and acceptor concentrations from freezeout statistics.

The van der Pauw technique was used to determine the Hall coefficient R_H and the carrier concentration n. The Hall measurement system at Tektronix was used for these measurements. Each sample was characterized electrically by analyzing Hall effect measurements as a

function of temperature. Gold-Ge contacts were applied to the samples and these were ohmic at all temperatures of interest.These measurements were made from 365 to 16 K in a magnetic field of 5 kG. Due to system constraints it was not possible to make measurements below 16 K. The carrier concentration n was calculated from the relation

$$n = r_H / R_H e \tag{4.1}$$

where r_H, the Hall coefficient factor, was assumed to be unity. Table II shows the result of Hall Measurement on nine different samples.

To determine the donor and acceptor concentration in samples which do not have sufficient carrier freezeout, the analysis of the temperature variation of the Hall coefficient or carrier concentration is not a reliable method. For GaAs this occurs for donor concentrations higher than about 5 x $10^{15}cm^{-3}$ [16]. In this work, the Brooks-Herring mobility formula was used to estimate N_D and N_A. The result for five different samples is shown in table III. An effective mass of $m^*/m = 0.072$ and a static dielectric constant of $\epsilon = 12.5$ were used in these calculations.

4.2. Results and Discussion

4.2.1. Growth Properties

Films upto 2.31 μm were grown at temperatures in the range 650-750 °C. Film surfaces were specular and free of apparent defects other than those attributable to contamination of the substrate surface. Any

TABLE II

OMVPE RUN #	MOBILITY ($cm^2 V^{-1} sec^{-1}$)		n (cm^{-3})	
	μ_{RT}	$\mu_{77 K}$	n_{RT}	$n_{77 K}$
79	2.640e3	1.133e4	2.407e16	9.963e15
80	3.009e3	8.259e3	1.726e16	1.142e16
81	1.794e3	1.848e3	1.583e18	1.504e18
82	2.373e3	2.346e3	3.089e17	2.811e17
83	2.855e3	2.929e3	2.328e17	2.046e17
96	1.899e2	1.664e3	3.993e16	9.494e15
100	1.835e3	7.817e3	2.384e16	8.901e15
108	3.745e3	1.111e4	4.217e15	2.930e15
112	1.632e3	1.413e3	2.491e17	2.272e17

TABLE III

OMVPE RUN #	N_D (cm^{-3})	N_A (cm^{-3})	N_A / N_D
79	2.907e16	5.005e15	0.172
80	3.300e16	1.574e16	0.477
96	1.343e17	9.439e16	0.703
100	3.580e16	1.196e16	0.334
108	1.475e16	1.053e16	0.714

contamination caused a localized hazy appearance which resulted from numerous microscopic hillocks. Depositions were made at 650 ° C, 680 ° C, and 750 ° C with a TMGa flow of 11.5-12.0 sccm and an arsine flow of 93-400 sccm. The range of growth rates seen in this study was 0.15 to 0.29 μm/min.

Film properties of undoped films were a strong function of deposition temperature, as has been observed at atmospheric pressure [36]. The electron Hall mobility measured at 77 K was greatest for films grown at 680 ° C.

Films were doped n-type with silicon by using silane. Carrier concentrations of up to 1.6 x $10^{18}cm^{-3}$ have been obtained. The electron concentration increased approximately linearly with silane flow rate (fig. 1). Silicon as a donor is on the gallium sub-lattice and under equlibrium conditions its incorporation should be proportional to the concentration of gallium vacancies, V_{GA} [37]. The doping reaction is:

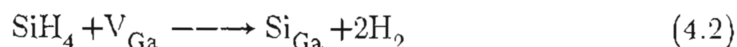

$$SiH_4 + V_{Ga} \longrightarrow Si_{Ga} + 2H_2 \qquad (4.2)$$

According to the model, as the arsine concentration is increased, the gallium vacancy concentration increases and therefore the silicon donor level should also increase. Conversely as the arsine concentration decreases, the arsenic vacancies should increase. The fact that the reverse behaviour takes place suggests that the incorporation of silicon

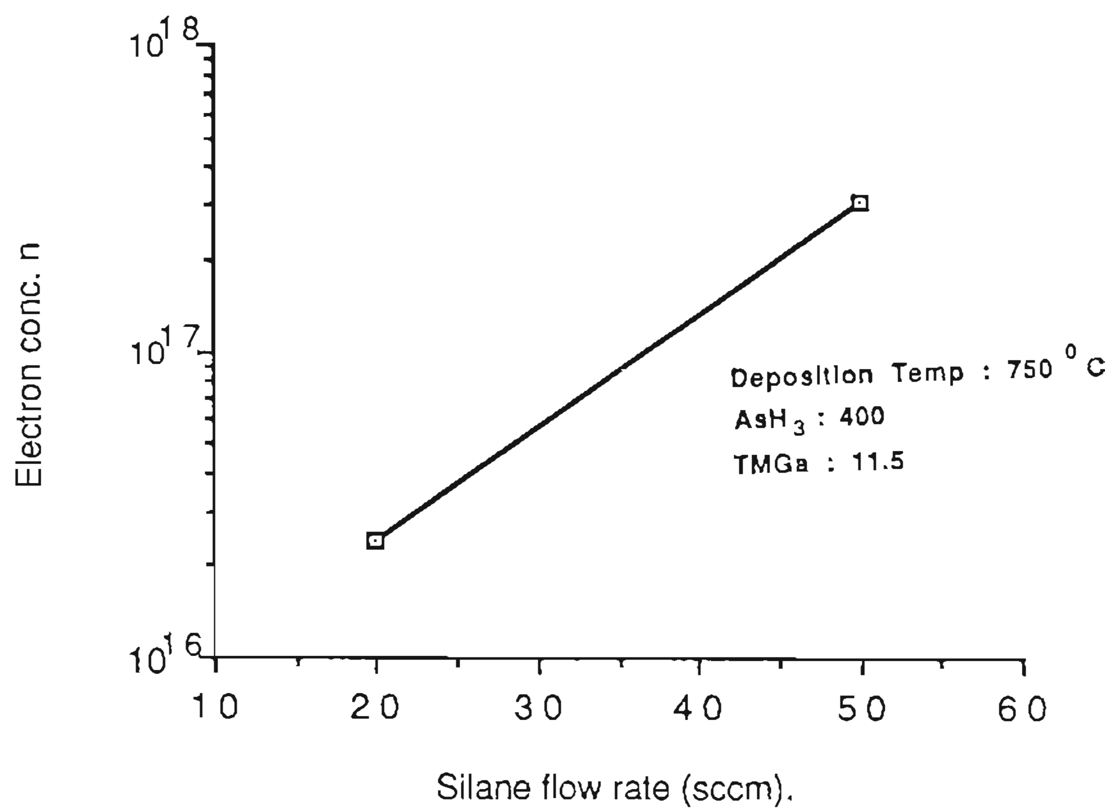

Fig. 1. Electron conc. in films doped with Si by using silane.

is not controlled by the bulk thermodynamic properties of the lattice but by a surface kinetic process; the arsenic appears to block the silicon from the growing surface. There was no indication from mobility values (fig.2) of any appreciable compensation of the donors by silicon acceptors.

There is a strong dependence of electron concentration with growth temperature (fig. 3). A 100°C drop in the growth temperature decreases the doping level by a factor of ten. Using the standard thermodynamic inverse temperature axis, the result can be expressed as

$$\log n = 26.57 - 8985/T \qquad (4.3)$$

over the temperature range 750 - 650°C [38]. The large change of electron concentration with growth temperature is probably a critical factor in obtaining uniform and reproducible doping levels.

It was observed that for high arsine levels, n-type material is produced and at low arsine levels the grown material is p-type. It has been suggested that this behaviour could be accounted for by the presence of a group IVb impurity, possibly silicon [9] The behaviour of silicon doping with arsine concentration would eliminate silicon as the major residual impurity. This would suggest that the behaviour is due to an intrinsic impurity such as carbon although there are probably other impurities involved also.

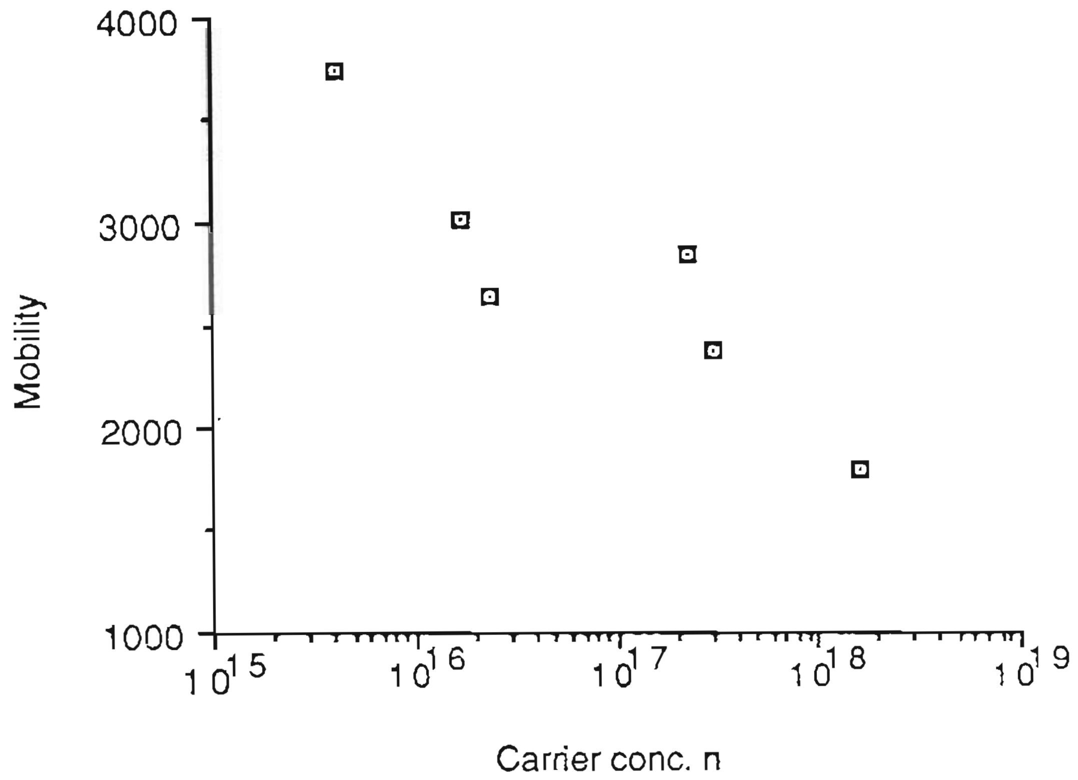

Fig. 2. Electron mobility for silicon doping.

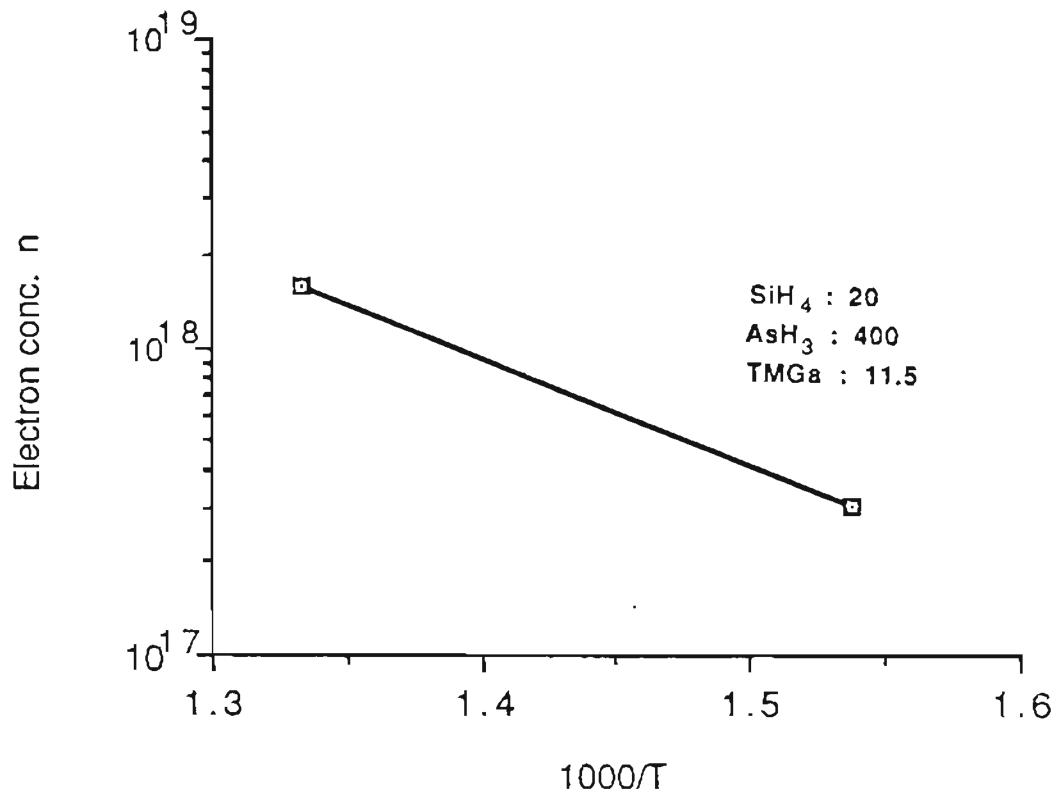

Fig. 3. Electron concentration as a function of temperature for silicon doping.

The experimental mobility measured at 5 kG for sample 108 is shown in Fig. 4. along with the mobility to be expected for the various scattering mechanisms. It can be seen that at low, intermediate, and higher temperatures the mobility is dominated by ionized impurity, piezoelectric, and polar optical scattering, respectively.

The experimental mobility variation for two different samples is shown in fig. 5. In compensated material the total number of ionized impurities is larger than the electron concentration, so that the mobility is lower than what would be expected for uncompensated material. Walukiewicz et al. [20] have computed the values of electron mobility in n-type GaAs at 77 K as a function of the carrier concentration and compensation ratio. For a given mobility and carrier concentration at 77 K, the values obtained for the compensation ratio in the present work closely match with their results. The results are shown in table IV.

Fig. 6 shows the temperature dependence of experimental mobility for samples 81 and 83. These samples were grown under similar conditions, except for temperature (sample 81: T = 750 °C, sample 83: T = 650 °C). Sample 81 had a room temperature mobility of 1.794×10^3 while sample 83 had 2.855×10^3. It is important to note here that an increase in temperature during the growth of GaAs results in an increase in the formation of both gallium and arsenic vacancies and a consequent

increase in the contaminant incorporation. The incorporation of carbon at higher growth temperatures should be considered in comparing these samples.

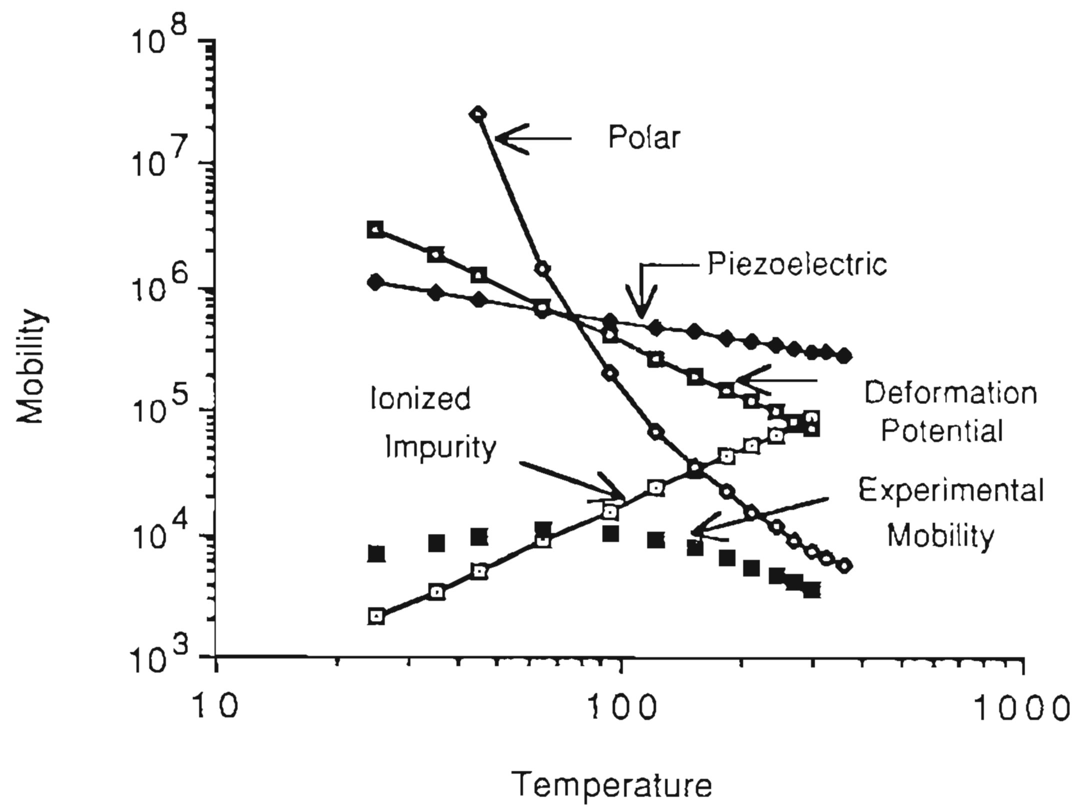

Fig. 4. Experimental temperature variation of the mobility of sample 108

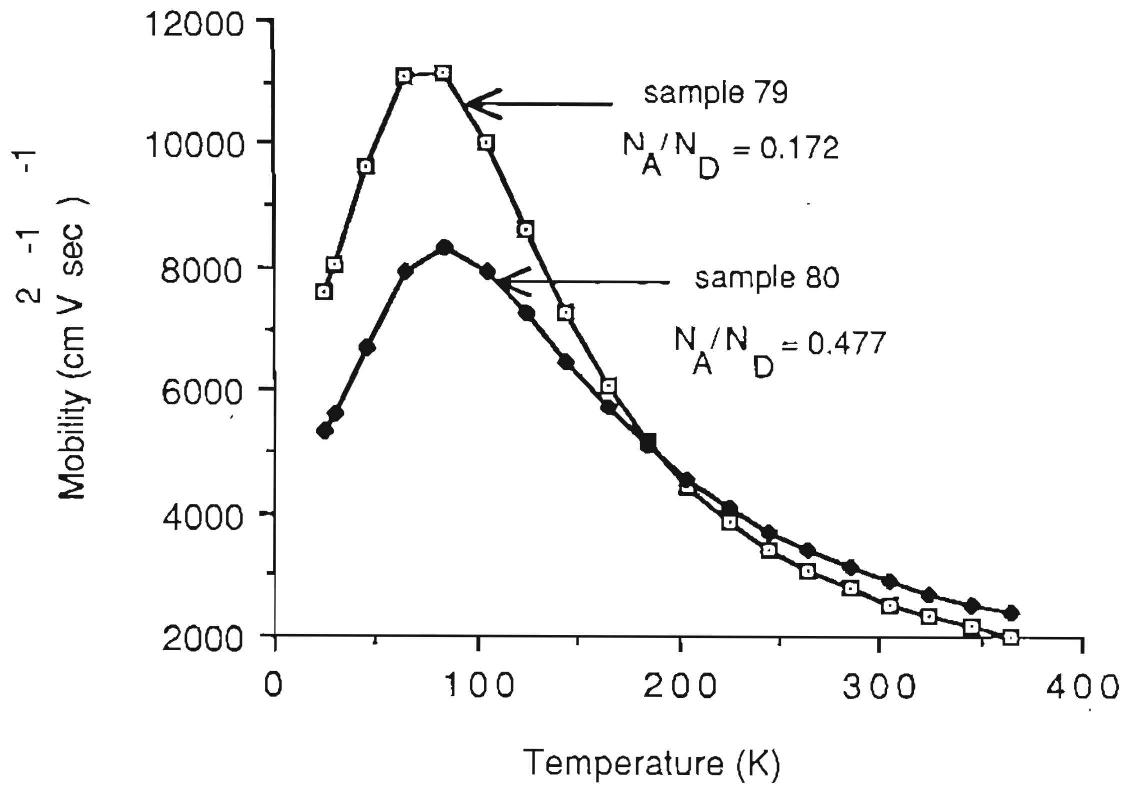

Fig. 5. Temperature dependence of experimental mobility.

TABLE IV

OMVPE RUN #	N_A / N_D	μ_{77K} (*)	μ_{77K} (†)
79	0.172	1.133e4	2.00e4
80	0.477	8.259e3	9.07e3
100	0.334	7.817e3	1.78e4
108	0.714	1.111e4	1.13e4

(*) ⟶ Present work

(†) ⟶ Walukiewicz et al.

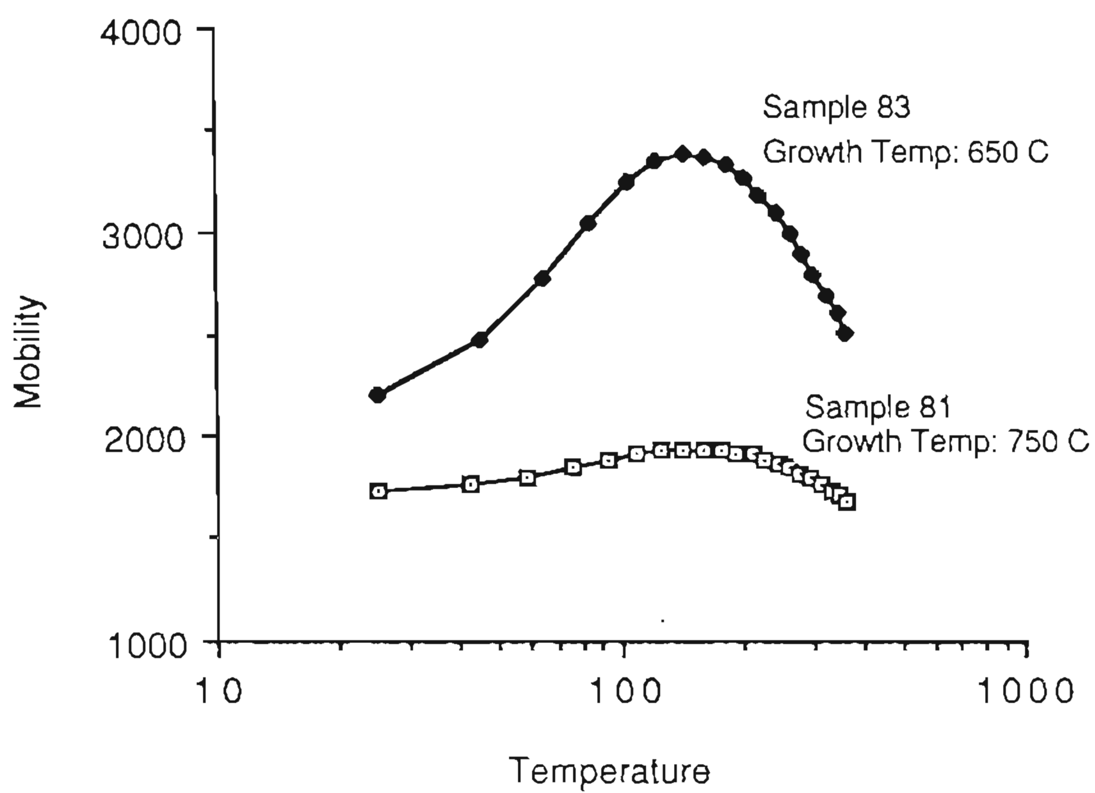

Fig. 6. Variation of mobility as a function of temperature.

CHAPTER 5

Conclusion

We have shown that GaAs of good quality can be grown by MOCVD at atmospheric pressure. The dependence of film properties on growth parameters is in agreement with that reported for atmospheric pressure experiments.

The doping of GaAs with silicon was studied as a function of temperature and of the concentration of silane. Silicon is always a donor and its incorporation is controlled by kinetic and not thermodynamic factors. Films could be reproducibly doped n-type in the range $10^{16}-10^{18}$ electrons/ cm^3 with silane.

Experimental studies of the room temperature electron mobility have been carried out on n-type GaAs. Calculations of the concentrations of ionized donor and acceptor impurities (N_D and N_A), and hence the total ionized impurity content, in epitaxial layers of GaAs, have been carried out using measurements of the free electron concentration (N_D - N_A) and Hall mobility at 77 K and the Brooks-Herring theory. Values of $m^* = 0.072$, $\epsilon = 12.5$ were used in these calculations. The largest errors in the values of ionized impurity density, determined in this manner, result from experimental errors, variations in scattering factor

with temperature and concentration. Experimental errors are typically less then about ±10%. The calculated scattering factor [39] for ionized impurity scattering varies from 1.29 at high concentrations and measurement temperatures to 1.60 at low concentrations and temperatures. For a magnetic field of 5 kG, the assumption that $r_H = 1$ results in a smaller underestimate of the carrier concentration.

The ionized impurity and lattice mobilities were combined by reciprocal addition. Although such an approximate method can lead to errors when applied over a wide range of values and temperature, they do give valid answers in regions where ionized impurity scattering is dominant. Such is the situation at 77 K in the range $5 \times 10^{15} < (N_D + N_A) < 10^{17}$ which was the region of interest in this study.

REFERENCE

[1] H. M. Manasevit and W. I. Simpson, *J. Electrochem. Soc.*, Vol. 116, pp. 1725 , 1969.

[2] H. M. Manasevit, *J. Cryst. Growth* , Vol. 55, pp. 1, 1981.

[3] H. M. Manasevit, *Appl. Phys. Lett.*, Vol. 12, pp. 156, 1968.

[4] H. M. Manasevit, F. M. Erdmann and W. I. Simpson, *J. Electrochem. Soc.*, Vol. 118, pp. 1864, 1971.

[5] H. M. Manasevit and W. I. Simpson, *J. Electrochem. Soc.*, Vol. 118, pp. C291 , 1971.

[6] H. M. Manasevit, *J. Cryst. Growth* , Vol. 22, pp. 125, 1974.

[7] P. R. Choudhury, *J. Electrochem. Soc.*, Vol. 116, pp. 1745 , 1969.

[8] W. R. Thomas, *J. Electrochem. Soc.*, Vol. 116, pp. 1450 , 1970.

[9] S. Ito, T. Shinohara and Y. Seki, *J. Electrochem. Soc.*, Vol. 120, pp. 1419 , 1973.

[10] Y. Seki, K. Tanno, K. Lida and E. Ichiki, *J. Electrochem. Soc.*, Vol. 122, pp. 1108 , 1975.

[11] J. M. Brown, N. Holonyak,Jr., M. J. Ludowise, W. T. Dietze and C. R. Lewis, *Electron. Lett.* , Vol. 20, pp. 204 , 1984.

[12] P. Frijlink and J. Maluenda, *Jpn. J. Appl. Phys.*, Vol. 21, pp. L574 , 1982.

[13] R. J. M. Griffiths, N. G. Chew, A. G. Cullis and G. C. Joyce, *Electron. Lett.* , Vol. 19, pp. 988 , 1983.

[14] T. Nakanisi, T. Udagawa, A. Tanaka and K. Kamei, *J. Cryst. Growth* , Vol. 55, pp. 255, 1981.

[15] F. C. Eversteijn, P. J. W. Severin, C. H. J. Brekel and M. L. Peek, *Electrochem. Soc.* , Vol. 117, pp. 925 , 1970.

[16] G. E. Stillman and C. M. Wolfe, *Thin Solid Films.* , Vol. 31, pp. 69 , 1976.

[17] B. R. Nag, *Electron Transport in Compound Semiconductors* . Springer, New York , 1980.

[18] C. M. Wolfe, G. E. Stillman and J. M. Dimmock, *J. Appl. Phys.* , Vol. 41(2) , pp. 504 , 1970.

[19] W. Walukiewicz, L. Lagowski, L. Jastrzebski, M. Lichtensteiger and H. C. Gatos, *J. Appl. Phys.* , Vol. 50(2) , pp. 899 , 1979.

[20] W. Walukiewicz, L. Lagowski and H. C. Gatos, *J. Appl. Phys.* , Vol. 53(1) , pp. 769 , 1982.

[21] D. L. Rode, *Semiconductors and Semimetals* . Vol. 10, New York: R. K. Willamson and A. C. Beer , 1975.

[22] D. Chattopadhyay and H. J. Queisser, *Rev. Mod. Phys.*, Vol. 53(4) , pp. 745 , 1981.

[23] H. Brooks, Advances in Electronics and Electron Physics , Vol. 7, 1955, pp. 85 .

[24] F. J. Reid, *Compound Semiconductors* . Vol. I , R. K. Willardson and H. L. Goering. pp. 158

[25] C. S. Kang and P. E. Greene, *Appl. Phys. Lett.* , Vol. 11 , pp. 171 , 1967.

[26] E. Andre and J. M. L. Duc, *Mater. Res. Bull.* , Vol. 3 , pp. 1 , 1968.

[27] D. V. Eddolls, *Phys. Status. Solidi* , Vol. 17 , pp. 67 , 1966.

[28] A. H. Wilson, *The Theory Of Metals* . Cambridge University Press, London, 1954. pp. 236

[29] D. E. Bolger, J. Franks, J. Gordon and J. Whitaker, *Proc. Int. Symp. on GaAs* . Inst. Phys. and Phys. Soc., London, 1967. pp. 16

[30] J. Whitaker and D. E. Bolger, *Solid State Commun.,* , Vol. 4 , pp. 181 , 1966.

[31] G. E. Stillman, C. M. Wolfe and J. O. Dimmock, *Proc. 3rd Photoconductivity Conf.,* . E. M. Pell (ed.), Pergamon Press, New York , 1971. pp. 265

[32] H. Ehrenreich, *Phys. Rev.* , Vol. 120, pp. 1960, 1951.

[33] J. Bardeen and G. L. Pearson, *Phys. Rev.* , Vol. 75, pp. 865, 1949.

[34] C. Erginsoy, *Phys. Rev.* , Vol. 79, pp. 1013, 1950.

[35] W. Shockley and J. Bardeen, *Phys. Rev.* , Vol. 80, pp. 72, 1950.

[36] P. D. Dapkus, H. M. Manasevit, K. L. Hess, T. S. Low and G. E. Stillman, *J. Cryst. Growth* , Vol. 55, pp. 10, 1981.

[37] R. F. Brebrick, *J. Appl. Phys.*, Vol. 33, pp. 422, 1962.

[38] S. J. Bass, *J. Cryst. Growth* , Vol. 47, pp. 613, 1979.

[39] A. C. Beer, *Galvanomagnetic Effects in Semiconductors..* Academic Press Inc., New York , 1963. pp. 111

APPENDIX A

Detailed Derivation of Equation (3.2)

General Equations

Consider a non-degenerate n-type semiconductor with a shallow donor concentration N_D and acceptor concentration N_A, the acceptors are fully ionized at all temperatures of interest. Let n_o be the concentration of free electrons in the conduction band.

The charge neutrality equation is given by:

$$p_0 + N_D^{\ +} = n_0 + N_A^{\ -} \tag{A.1}$$

$$N_D^{\ +} = n_0 + N_A - p_0 \quad (N_A^{\ -} = N_A \text{: all acceptors ionized })$$

The ionized donor concentration is given by:

$$N_D^{\ +} = N_D \left[1 - \frac{1}{1 + \beta \exp\left(\dfrac{E_D - E_F}{kT} \right)} \right] \tag{A.2}$$

Therefore,

$$N_D \left[1 - \frac{1}{1 + \beta \exp\left(\frac{E_D - E_F}{kT}\right)} \right] = n_0 + N_A - p_0 \tag{A.3}$$

Rearranging the above equation results in the following equation:

$$\beta \exp\left(\frac{E_D - E_F}{kT}\right) = \frac{N_A + n_0 - p_0}{N_D - N_A - n_0 + p_0} \tag{A.4}$$

The free carrier concentration in the conduction band is defined by

$$n_0 = N_c \exp\left(-\frac{E_C - E_F}{kT}\right) \tag{A.5}$$

Thus,

$$\frac{N_C}{n_0} = \exp\left(\frac{E_C - E_F}{kT}\right) \tag{A.6}$$

Next consider,

$$\begin{aligned} E_D - E_F &= E_D - E_F + E_C - E_C \\ &= (E_D - E_C) + (E_C - E_F) \end{aligned}$$

Therefore,

$$\exp\left(\frac{E_D - E_F}{kT}\right) = \exp\left(\frac{E_D - E_C}{kT}\right) \exp\left(\frac{E_C - E_F}{kT}\right)$$

$$= \frac{N_C}{n_0} \exp\left(\frac{E_D - E_C}{kT}\right)$$

Substituting the above equation into equation (A.4) gives

$$\beta \frac{N_C}{n_0} \exp\left(\frac{E_D - E_C}{kT}\right) = \frac{n_0 + N_A - p_0}{N_D - N_A - n_0 + p_0} \qquad (A.7)$$

$$\frac{n_0\left(n_0 + N_A\right) - n_0 p_0}{N_D - N_A - n_0 + p_0} = \beta N_C \exp\left(\frac{E_D - E_C}{kT}\right)$$

Since the conduction band is the reference level, one can write

$$E_D - E_C = -(E_C - E_D) = -E_D \qquad (A.8)$$

$$\frac{n_0(n_0 + N_A) - n_i^2}{N_D - N_A - n_0 + p_0} = \beta N_C \exp\left(\frac{-E_D}{kT}\right)$$

$$\frac{n_0(n_0 + N_A) - n_i^2}{N_D - N_A - n_0 + (n_i^2/n_0)} = \frac{N_C}{g_1} \exp\left(\frac{-E_D}{kT}\right) \qquad (A.9)$$

APPENDIX B

Detailed Derivation of Equation (2.8)

Brooks-Herring Ionized Impurity Mobility

Consider a singly ionized impurity atom of charge Ze fixed inside the crystal, as a scattering center. The electron drift orbit is a hyperbola with the ion in one of its focal points depending on the sign of the electronic charge.

The distance between the ion and the asymptote is called the "impact parameter". For convenience, let this distance be denoted by κ , where,

$$\kappa = \frac{Ze^2}{4\pi\epsilon\epsilon_0 mv^2} \tag{B.1}$$

Since the total scattering cross-section of a coulomb charge diverges due to the long-range character of the potential, proper care should be taken in screening the bare charge or introducing otherwise suitable cutoffs.

The approach of Brooks and Herring consists of letting the carriers and ionized impurities redistribute themselves in such a way so as to produce mutual screening.

Consider the following potential,

$$V(r) = -\frac{Ze}{4\pi\epsilon\epsilon_0 r} e^{-r/L_D} \tag{B.2}$$

In order to calculate the differential scattering cross-section, the Hamiltonian Matrix element $M_{k'k}$ needs to be calculated first.

$$M_{k'k} = \int \psi_{k'}^{*} eV(r) \psi_k d^3\vec{r} \tag{B.3}$$

where, $\psi_k = V^{-1/2} e^{i\vec{k}.\vec{r}}$

$$M_{k'k} = \frac{e}{V}\int V(r) e^{i(\vec{k}-\vec{k}').\vec{r}} d^3\vec{r}$$

$$= \frac{e}{V}\int_0^{2\pi}\int_0^{\pi}\int_0^{\infty} V(r) e^{i(\vec{k}-\vec{k}')r\cos\theta} r^2 \, dr \sin\theta \, d\theta \, d\phi$$

$$= \frac{e}{V} 2\pi \int_0^{\infty} V(r) r^2 \int_0^{\pi} e^{iqr\cos\theta} \sin\theta \, d\theta \, dr$$

where, $q = |\vec{k}-\vec{k}'|$

$$M_{k'k} = \frac{e}{V} 4\pi \int_0^{\infty} V(r) r^2 \frac{\sin qr}{qr} dr$$

Inserting value of V(r) from equation (B.2) into the above equation gives

$$M_{k'k} = -\frac{Ze^2}{V\epsilon\epsilon_0 q} \int_0^{\infty} e^{-r/L_D} \sin qr \, dr \tag{B.4}$$

The integral, $\int_0^{\infty} e^{-r/L_D} \sin qr \, dr = \frac{q}{q^2 + L_D^{-2}}$

Therefore,

$$M_{k'k} = -\frac{Ze^2}{V\epsilon\epsilon_0}\left[\frac{1}{q^2 + L_D^{-2}}\right]$$

Also, since $q = |\vec{k'}-\vec{k}| = 2k\sin(\theta/2)$

$$M_{k'k} = -\frac{Ze^2}{V\epsilon\epsilon_0 4k^2[\sin^2(\theta/2) + (2kL_D)^{-2}]} \qquad \text{(B.5)}$$

The differential scattering cross-section is given by

$$\sigma(\theta) = \left\{\frac{Vm}{2\pi h^2}|M_{k'k}|\right\}^2 \qquad \text{(B.6)}$$

$$= \left[\frac{Vm}{2\pi h^2}\frac{Ze^2}{V\epsilon\epsilon_0}\frac{1}{4k^2[\sin^2(\theta/2) + (2kL_D)^{-2}]}\right]^2$$

$$= \left[\frac{\kappa/2}{\sin^2(\theta/2) + (2kL_D)^{-2}}\right]^2$$

Next, the expression for the relaxation time is

$$\frac{1}{\tau(x)} = N_I v 2\pi\int_0^\pi \sigma(\theta)(1 - \cos\theta)\sin\theta\, d\theta \qquad \text{(B.7)}$$

$$= N_I v 2\pi\int_0^\pi \left[\frac{\kappa/2}{\sin^2(\theta/2) + (2kL_D)^{-2}}\right]^2(1-\cos\theta)\sin\theta\, d\theta$$

$$= \frac{\kappa^2}{2}N_I v \pi\int_0^\pi \frac{1}{\left[\sin^2(\theta/2) + (2kL_D)^{-2}\right]^2}(1-\cos\theta)\sin\theta\, d\theta$$

$$\int_0^{\pi} \frac{(1-\cos\theta)\sin\theta\, d\theta}{\left[\sin^2(\theta/2) + (2kL_D)^{-2}\right]^2} = \int_0^{\pi} \frac{(1-\cos\theta)\sin\theta\, d\theta}{\left[\frac{1-\cos\theta}{2} + (2kL_D)^{-2}\right]^2}$$

$$= 4 \int_0^{2} \frac{x\,dx}{\left[x + 2\beta^{-2}\right]^2}$$

where, $x = 1-\cos\theta$

$$d\theta \sin\theta = d(1-\cos\theta) = dx$$

and, $\beta=2kL_D$

Therefore,

$$\int_0^{\pi} \frac{(1-\cos\theta)\sin\theta\, d\theta}{\left[\sin^2(\theta/2) + (2kL_D)^{-2}\right]^2} = 4\left\{\ln(1 + \beta^2) - \frac{\beta^2}{1 + \beta^2}\right\} \qquad \text{(B.8)}$$

Substituting equation (B.8) into (B.7) gives

$$\frac{1}{\tau(x)} = N_I v \pi \frac{\kappa^2}{2} 4 \left\{\ln(1+\beta^2) - \frac{\beta^2}{1+\beta^2}\right\}$$

$$= N_I v \frac{\pi}{2} \left(\frac{Ze^2}{4\pi\epsilon\epsilon_0 m v^2}\right)^2 4 \left\{\ln(1+\beta^2) - \frac{\beta^2}{1+\beta^2}\right\}$$

$$= \left(\frac{Ze^2}{\epsilon\epsilon_0}\right)^2 \left(\frac{N_I}{16\pi}\right) \frac{1}{E^{3/2}} \frac{1}{\sqrt{2m}} \left\{\ln(1+\beta^2) - \frac{\beta^2}{1+\beta^2}\right\}$$

Thus,

$$\tau(x) = \left(\frac{\epsilon\epsilon_0}{Ze^2}\right)^2 \left(\frac{16\pi}{N_I}\right) \frac{E^{3/2}\sqrt{2m}}{\left\{\ln(1+\beta^2) - \dfrac{\beta^2}{1+\beta^2}\right\}} \tag{B.9}$$

Now, mobility is defined by the following expression

$$\mu_I = \frac{e}{m}\langle\tau\rangle$$

where,

$$\langle\tau\rangle = \frac{\int x^{3/2} e^{-x} \tau(x) dx}{\int x^{3/2} e^{-x} dx} \qquad x = \frac{E}{kT}$$

Now, from definition of gamma function

$$\int_0^\infty t^{n-1} e^{-t} dt = \Gamma(n) \qquad n>0$$

Hence, $\int x^{3/2} e^{-x} dx = \Gamma(5/2)$

Also, $\tau(x)$ is given by equation (B.9)

Therefore, the expression for $\langle\tau\rangle$ can be rewritten as

$$\langle\tau\rangle = \frac{\int x^{3/2} e^{-x} \tau(x) dx}{\Gamma(5/2)}$$

Now $\tau(x)$ in equation (B.9) above can be rewritten as

$$\begin{aligned} \tau(x) &= \tau_0 E^{3/2} \\ &= \tau_0 (kT)^{3/2} x^{3/2} \\ &= \tau_0' x^{3/2} \end{aligned}$$

where, $\tau_0 = \left(\frac{\epsilon\epsilon_0}{Ze^2}\right)^2 \left(\frac{16\pi}{N_I}\right)\sqrt{2m}\frac{1}{\left[\ln(1+b) - \frac{b}{1+b}\right]}$ and $b=\beta^2$,

$$\tau_0' = \tau_0(kT)^{3/2}$$

$$<\tau> = \tau_0' \frac{\Gamma(5/2+3/2)}{\Gamma(5/2)}$$

$$= \tau_0' \frac{8}{\sqrt{\pi}}$$

The expression for the ionized impurity mobility now reads as

$$\mu_I = \frac{e}{m}<\tau>$$

$$= \frac{e}{m}\left(\frac{\epsilon\epsilon_0}{Ze^2}\right)^2 \left(\frac{16\pi}{N_I}\right)\sqrt{2m}\frac{1}{\left[\ln(1+b) - \frac{b}{1+b}\right]}(kT)^{3/2}\frac{8}{\sqrt{\pi}}$$

$$= \frac{128(2\pi)^{1/2}\epsilon_0^2 k^{3/2}}{e^3 m_0^{1/2}} \frac{\epsilon^2 T^{3/2}(m_0/m^*)^{1/2}}{N_I\left[\ln(1+b) - \frac{b}{1+b}\right]}$$

Thus, the Brooks-Herring mobility formula for the ionized impurities is given by

$$\mu_I = 3.28x10^{15}\frac{(m_0/m^*)^{1/2}\epsilon^2 T^{3/2}}{N_I\left[\ln(1+b) - \frac{b}{1+b}\right]} \qquad \text{(B.10)}$$

$$b = \beta^2 = (2kL_D)^2$$

$$= \left[2k \sqrt{\frac{k_B T \epsilon \epsilon_0}{e^2 n}} \right]^2$$

$$= \left[2 \sqrt{\frac{2mE}{h^2}} \sqrt{\frac{k_B T \epsilon \epsilon_0}{e^2 n}} \right]^2$$

$$= \frac{24 m_0 k_B^{\,2} \epsilon_0}{h^2 e^2} \frac{(m^*/m) T^2 \epsilon}{n}$$

$$b = 1.294 \mathrm{x} 10^{14} \frac{(m^*/m) T^2 \epsilon}{n} \qquad (B.11)$$

VITA

The author was born on February 11, 1961 in Bombay, India. She received a Master of Science degree in Physics from the University of Bombay, India in 1982.

After graduation from college, she taught Physics at C.H.M College, India for six months. In December 1983, the author accepted a position as a Senior Scientist at Nehru Planetarium, Bombay, India, where she was involved in producing and directing a number of Planetarium sky-theater programmes, and audio-visual shows. During this time the author also took great interest in generating an awareness of science (and Astronomy in particular) in the common public via the media of Radio, Television and various science magazines.

In August of 1985, the author came to United States for graduate studies in Physics at Lousiana State University (LSU). After a year at LSU, the author moved to Oregon Graduate Center in September of 1986, to pursue a Masters Degree in the field of Electrical Engineering.